ISSN 2563-9218

RESEARCH ARTICLE

Protective Role of Quercetin on Silver Nanoparticle-Induced Hepatotoxicity in Sprague-Dawley Rats

Anita K Patlolla[1,2*], Sidney Graham[2,3], Paul B Tchounwou[4]

Patlolla AK, Graham S, Tchounwou PB. Protective Role of Quercetin on Silver Nanoparticle-Induced Hepatotoxicity in Sprague-Dawley Rats. Int J Biomed Clin Anal. 2024;4(2):52-64.

Abstract

Silver nanoparticles (Ag-NPs) are one of the most commercially used nanomaterials. However, their extensive usage has adverse biological effects, which has led to increasing concerns about their potential impact on human health and the environment. This study aimed to confirm Ag-NP-induced hepatotoxicity and determine the potential protective role of quercetin (Qur) in Ag-NP-induced hepatotoxicity. Fifteen healthy male Sprague-Dawley rats were divided into three group: (1) Control group (administered deionized water), (2) Ag-NPs group (administered 100 mg/Kg Ag-NP orally) and (3) Ag-NP+Qur group (administered 100 mg/Kg Ag-NPs+100 µl of Qur) for five consecutive days. Samples were collected 24 h after the last treatment following standard protocols. The antioxidant activity of Qur against Ag-NP-induced toxicity was determined by measuring serum levels of various enzymes including Alanine Aminotransferases (ALT), Gamma-Glutamyl Transferases, (GGT), Alkaline Phosphatases (ALP), biomarkers of oxidative stress, Malondialdehyde (MDA), reduced glutathione (GSH) and examining liver histopathology. A significant increase in the activity of serum liver enzymes (ALT, ALP, GGT), MDA and alterations in liver morphology were noted in Ag-NPs treated rats relative to control rats. In contrast, reduced glutathione level was considerably lower in Ag-NPs treated rats compared to that in control rats. Co-administration of Qur resulted in significant changes in the biochemical parameters compared to that in Ag-NP-treated rats. The activity of liver enzymes, liver injury and oxidative stress biomarkers were found to be decreased, whereas levels of reduced glutathione were increased in the Qur+Ag-NP group. Our results suggest that the antioxidant Qur may have a protective role against Ag-NP-induced hepatotoxicity.

Key Words: *Silver nanoparticles; Quercetin; Hepatotoxicity; Alanine aminotransferases; Gamma-glutamyl transferases; Alkaline phosphatases; Malondialdehyde; Reduced glutathione; Rats*

1NIH-Center for Environmental Health, College of Science Engineering and Technology, Jackson State University, Jackson, MS-39217, USA

2Department of Biology, CSET, Jackson State University, Jackson, MS-39217, USA

3The Aristocrats STEM & Health Science Program, Jackson State University, Jackson, 39217, USA

4Morgan State University, Baltimore, Maryland, USA

[*]Corresponding author: Anita K Patlolla, Assistant Professor, Department of Biology, CSET, Jackson State University, 1400 Lynch Street, PO. Box 18540, Jackson, MS-39217, USA, E-mail: anita.k.patlolla@jsums.edu

Received: October 09, 2024, Accepted: October 27, 2024, Published: November 07, 2024

Introduction

Silver Nanoparticles (Ag-NPs) are among the most commercialized nanomaterials worldwide. Given its application in a wide variety of products, we evaluated the potential toxicity of Ag-NPs in cells, tissues and organs. Exposure to Nanoparticles (NPs) can occur *via* water, food, drugs and cosmetics and cause various toxicological effects. As the use of Ag-NPs in consumer and medical applications continues to increase, people are at high risk of exposure to Ag-NPs in daily life through occupational exposure and consumer products. Therefore, the adverse effects of Ag-NPs on human health and the environment are of increasing concern [1]. The potential damage caused by NPs to organs and systems in the body has been reported previously, which may affect the biomedical application of NPs [2]. Therefore, it is necessary to evaluate the dynamics of Ag-NPs *in vivo* [3,4]. Ag-NPs enter the body through various routes, including inhalation, ingestion, dermal contact and intravenous injection and are subsequently distributed to different organs. Owing to their small size, Ag-NPs can easily penetrate the body and cross barriers such as the blood-brain barrier and subsequently induce toxicity. In addition to direct tissue exposure, Ag-NPs are also transported to various organs *via* blood circulation [5].

Liver is a major site for detoxification, metabolism and biotransformation of xenobiotics including nanoparticles [6]. Hepatocytes are targets for Reactive Oxygen Species (ROS) since most chemicals are metabolized in the liver as well as one of the most often attacked organ. Normally hepatotoxicity detections methods vary with the circumstances of their use. In this case, demonstrating a physiologically significant adverse effect requires *in vivo* studies. Biochemically, serum enzyme analyses have become the standard measure of hepatotoxicity during the past 25 years [7]. Measurement of enzyme activities in serum permit detection of hepatotoxicity with far less labor than that required for other tests. The rationale for the use of serum transaminases and other enzymes is that these enzymes, normally contained in the hepatocytes, gain entry into the general circulation after cellular injury [8]. Therefore, hepatocytes are broadly studied in liver toxicity of Ag-NPs. Acute hepatobiliary injury in mice, including remarkable necrosis of hepatocytes and hemorrhage in gall bladder was reported by [9]. Additionally, in this study acute hepatobiliary injury induced by Ag-NPs were found to be size and dose dependent. Small size of Ag-NPs caused severe toxic effects and high dose produced deleterious hepatobiliary injury. Multi-system acute toxicities in mice with a single intravenous injection of Ag-NPs was observed by Recordati et al [10]. The results of Recordati et al study occurred in two phases, in the first phase remarkable hepatobiliary damage were reported including hepatocyte necrosis, micro hemorrhage around the biliary duct and portal vein injury. In the second phase acute tubular necrosis and apoptosis and moderate splenomegaly were observed in Ag-NPs exposed mice. Ag-NPs penetrating through skin in a study by Heydarnejad et al observed time-dependent liver damage such as hyperemia, dilatation in central venous, swelling hepatocytes and increased inflammatory cells [11]. In addition to hepatocytes, Kupffer Cells (KC) play a significant role in the liver physiology and homeostasis as it is a resident macrophage including in removal of nanoparticles from organisms. Hence, KCs are important focus of research on liver toxicity and metabolism of Ag-NPs [12].

A large variety of plants are cultivated globally for food and medicinal purposes. Several traditional medicinal plants with antioxidant properties have been used to treat various ailments. of health problems. Plant-based

antioxidants have been extensively studied for the prevention and treatment of oxidative stress induced by NP toxicity. Phytochemicals with high antioxidant potential are often used as protective agents in studies on NP-induced toxicity [13]. These include Quercetin (Qur), a natural flavonoid that occurs abundantly in many fruits, vegetables and medicinal plants. Its antioxidant and anti-inflammatory/antiallergic properties are well documented. Qur inhibits the release of histamine and other inflammatory mediators in the body. The bioactivity of Qur is related to its high antioxidant activities [14,15]. The protective role and antioxidant activity of Qur has been evaluated in different models following exposure to TiO_2-NP, AuNPs, CuO-NP and ZnO-NP. Quercetin exhibited antioxidant-mediated protection in the liver, kidney and testicular tissues of rats exposed to TiO_2-NP and hepatoprotective activity in AuNP intoxicated rat liver [14,16,17]. Similar Qur-mediated antioxidant protection against CuO-NP-induced and ZnO-NP-induced hepatotoxicity has been previously reported in rats [18,19]. However, no study has evaluated the protective effect of Qur against Ag-NP-induced toxicity. Therefore, the objective of the present study was to confirm the hepatotoxic effects of Ag-NPs and assess the protective role of Qur against Ag-NP-induced hepatotoxicity in rats.

Materials and Methods

Chemicals

Ag-NPs in liquid form (10 nm diameter) were purchased from Ocean Nanotech, LLC. (Fayetteville, Arkansas, USA). Quercetin, Xylene, thioalcohol, paraffin wax, hematoxylin-eosin stain and diagnostic kits for serum Alanine Aminotransferase (ALT), Gamma-Glutamyl (GGT) and alkaline phosphatase were obtained from Sigma-Aldrich (St. Louis, MO, USA). Lipid peroxidation kits were purchased from Calbiochem (La, Jolla, CA, USA).

Test system and treatment

Ag-NPs were mixed in deionized water (DI-water) and dispersed by ultrasonic vibration (100 W, 30 kHz) for 30 min to make a stock solution of 50 µg/ml. The Ag-NP dose was selected according to the results obtained in our previous studies where we used 5,25,50 and 100 mg/kg Ag-NPs and demonstrated that 100 mg/kg Ag-NPs exhibited the highest toxicity in most of the organs of the rats, which was confirmed by histological investigations [20]. Qur doses was 100 mg/kg, which were selected according to preliminary studies in our laboratory.

Characterization of Ag-NPs

Transmission Electron Microscope (TEM) was used to determine the size, shape and morphology of the silver nanoparticles. The samples of sonicated pellet of centrifuged Ag-NPs in deionized water were used for TEM analysis. On a carbon-coated copper grid, a drop of the homogenous suspension was placed with a lacey carbon film and allowed to dry at room temperature. The images were collected using a field emission JOEL-JEM-2100F TEM operating at 200kv (JOEL-Tokyo, Japan) (Figure 1).

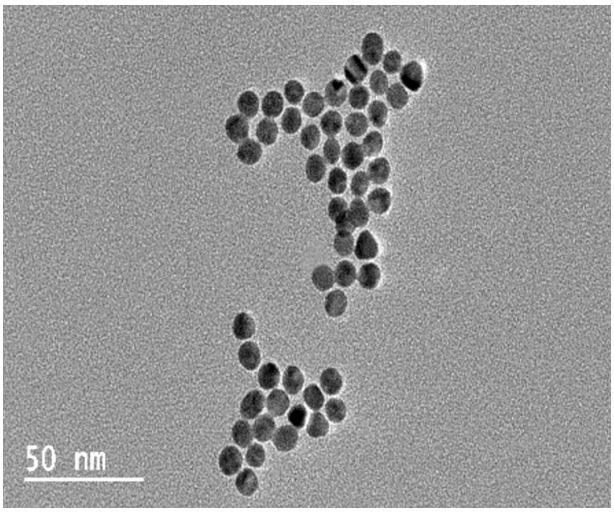

Figure 1) *Transmission electron microscope image of silver nanoparticle.*

Nanostructure size and zeta potential were measured in deionized water (DI water) using a Zetasizer (Malvern, Worcestershire, UK) (Figure 2). Briefly, the nanoparticle samples were measured after dilution of an Ag-NP stock solution of 50 µg/ml in water. These dilutions were vortexed and sonicated for 5 min to provide a homogenous dispersion. For the size measurement, 1 ml of the diluted dispersion Ag-NPs was transferred to a 1 cm^2 cuvette for dynamic size measurement (Figure 2A). For zeta potential measurement, a Malvern zeta potential cell was washed 3-4 times with ultrapure water followed by transferring 850 µl of diluted dispersion Ag-NPs to this cell to measure the zeta potential (Figure 2B). To assure the quality of the data the concentration of the samples and experimental methods were optimized. Sixty nm NIST standard gold nanoparticles were used in the validation of the instrument. Both size and zeta potential were measured at least three times. The data were calculated as the average size or zeta potential of Ag-NPs.

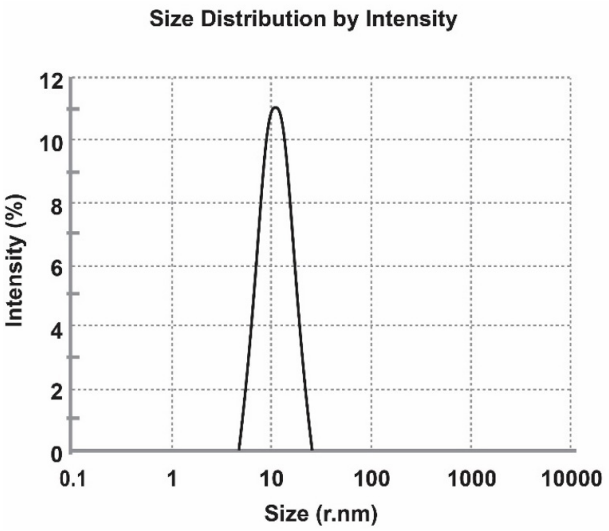

Figure 2A) *Ag-NPs size (10 nm) by intensity.*

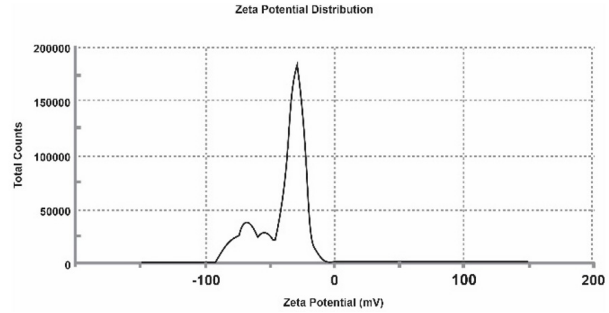

Figure 2B) *Zeta potential of Ag-NPs.*

Animals

Fifteen healthy adult male Sprague-Dawley rats (8-10 weeks of age, average body weight (BW) of 125 ± 2 g) were obtained from Harlan-Sprague-Dawley Breeding Laboratories in Indianapolis, Indiana, USA. The rats were randomly selected and housed in polycarbonate cages (18.88 in x 7.25 in x 3.76 in) (five rats per cage) with steel wire tops and corn-cob bedding. They were maintained in a controlled atmosphere with a cyclic 12 h dark/12 h light cycle, a temperature of 25°C and 50%-70% humidity and with free access to pelleted feed (oval normal diet with complete balanced nutritional value for biomedical research) and fresh tap water. The rats were allowed to acclimate for 10 days before treatment.

Experimental design

The rats were allowed to fast (fasting involves maintenance of homeostasis while relying on endogenous resources) 24 hours prior to administration of the Ag-NPs and then divided into three groups of five rats each. The first group (I) served as a control and were administered deionized water only. The second group (II) was administered a daily oral dose of 100 mg/Kg of 10 nm Ag-NP for 5 days. The third group (III) was administered a daily oral dose of 100 mg/Kg of 10 nm of Ag-NPs along with 100 µl of Qur for 5 days. This study was approved by the local Ethics committee for animal experiments (Institutional Animal Care and Use Committee) at Jackson State University, Jackson MS, (USA). The experiment was conducted in accordance with the directive 86/609/EEC on the protection of laboratory animals [21]. All procedures involving animals and their care complied with the institutional guidelines and the national and international laws and guidelines for the use of animals in biomedical research [22].

Preparation of liver homogenates

Liver samples were excised under anesthesia after 24 h at the end of the 5 days of treatment. The samples were thoroughly washed with ice-cold physiological saline and weighed. Liver homogenate (10%) was prepared in 0.05 M phosphate buffer (pH 7.4) containing 0.1 mM EDTA using a Teflon-pestle homogenizer (Fischer, Hampton, NH, USA), followed by sonication (Branson SFX250 Sonifier, Marshell Scientific, Hampton, NH, USA) and centrifugation at 500 x g for 10 min at 4°C. The supernatant was drained and centrifuged again at 2000 x g for 1 h at 4°C. The resulting cellular fraction constituted the liver homogenate, which was used for the assays.

Biochemical analysis

Blood samples were collected directly after anesthetization using heparinized syringes and transferred to polypropylene tubes. The samples were allowed to clot for a minimum of 30 min (maximum 60 min). After clotting, the samples were centrifuged at 750 x g for 10 min. The serum was separated from the cellular fraction (erythrocytes, platelets, leucocytes) by pipetting and transferred to an acid-washed polypropylene tube, labeled and stored at 4°C until analysis. The activities of liver enzymes, including ALT/GPT, GGT and ALP in the serum samples were determined using colorimetric assay kits.

Enzyme analysis

Serum aminotransferases: Human serum contains several distinct transaminases. The two most assayed markers in clinical practice are ALT/GPT and GGT. The activities of ALT/GPT and GGT in the serum were determined using a previously described protocol with slight modifications [23]. Catalytic reaction of these enzymes involves transfer of alpha amino groups from specific amino acids to Alpha-Ketoglutaric acid (AKG) to produce glutamic acid and oxaloacetic or pyruvic acid. The resulting keto acids are calorimetrically determined after reaction with 2, 4-Dinitrophenyl hydrazine (DNP). The absorbance of the mixture resulting from the between the hydrazones of AKG, oxaloacetic acid and pyruvic acid was measured at 505 nm.

Determination of GPT/ALT: A prepared solution of alanine α-KG substrate (1.0 mL) was pipetted out into test tubes corresponding to Ag-NP, Ag-NP + Qur and control samples and placed in 37°C water bath. Next, 0.2 ml serum was added to the tube, mixed by gently shaking and incubated in the water bath. Sigma color reagent (1.0 mL) was added exactly 30 min after the addition of serum, gently agitated and left at room temperature (25°C) for 20 min. Sodium hydroxide solution (10 mL of 0.40 N NaOH) was then added to the reaction mixture, mixed by inverting the tube and incubated at room temperature (25°C) for an additional 5 min. The absorbance was read at 505 nm and a calibration curve was prepared using water as a reference. GPT activity was determined in Sigma Frankel (SF) units/mL from the corresponding readings on the calibration curve.

Determination of Gamma-Glutamyl Transferase (GGT): The GGT in sample recognizes L-γ-Glutamyl-pNA a specific substrate, leading to color development proportional to the amount of GGT. GGT activity can thus be quantified using a colorimetric assay (λ=418 nm). The manufacturer's (Sigma-Aldrich, St. Louise, MO, USA) protocol was used to determine GGT activity in rat liver samples.

Alkaline phosphatases: ALP activity in serum was determined using the method described by Kay et al. with slight modification [24]. ALP depends on the hydrolysis of p-nitrophenyl

phosphate by the enzyme, which yields p-nitrophenol and inorganic phosphate. Under alkaline conditions, p-nitrophenol is readily converted into a yellow complex, which is measured at wavelength of 400-420 nm. The intensity of color formed is proportional to phosphatase activity.

The reaction for ALP is as follows:

$$\text{Orthophosphoric monoester} + H_2O \xrightarrow{\text{ALP}} \text{alcohol} + H_3PO_4$$

Alkaline phosphatases: Serum ALP activity was measured using the following steps were conducted. Test tubes (15 mL) were labeled as ‘‘Blank’’ or ‘‘Test’’ (control and treated samples). Alkaline buffer and stock substrate solution, (0.5 mL each) were pipetted in each test tube and the tubes were placed at 37°C in a water bath for equilibrium. Water (0.1 mL) or serum from the treated group (0.1 mL) were added to the tubes labeled ‘‘Blank’’ and ‘Test” respectively’. The time is recorded and samples are mixed gently and immediately replaced in the 37°C water bath. After 15 min, 10.0 ml of 0.05 N (Normal) sodium hydroxide (NaOH) was added to all the tubes and the contents were mixed by inverting the tubes. The absorbance of ‘‘Blank’’ (as reference) tubes versus “Test” tubes was read at 420 nm using a visible spectrophotometer (BIO-RAD, Hercules, CA). The first absorbance reading of the reaction mixture was used as the initial readings of ALP activity in serum. ALP units were determined from the corresponding calibration curve. Four drops of (approximately 0.2 mL) concentrated Hydrochloric acid (HCl) were added to each test tube and mixed. The absorbance of the ‘‘Blank’’ versus ‘‘Test’’ were read again. The recorded absorbances values were the final readings of the reaction mixture. The ALP activity was calculated by subtracting the final absorbance from the initial absorbance reading of the corresponding group.

Reduced glutathione (GSH): GSH activity was determined using the method described by Ellman [25]. Tissue homogenate, prepared in 0.1 M phosphate buffer, pH 7.4, was added to equal volume of 20% trichloroacetic acid (TCA) containing 1 mM Ethylenediamine tetra acetic acid (EDTA to precipitate the tissue proteins. The mixture was allowed to stand for 5 min and centrifuged at 2000 RPM for 10 min. An aliquot of tissue supernatant (50 µL) was mixed with 1.7 mL of disodium hydrogen phosphate solution (0.3 M). The final volume was adjusted to 2 mL by adding 250 µL of Ellman’s reagent (DTNB reagent-4 mg of 5, 5-dithiobis (2-nitro benzoic acid) in 10 mL of 1% (w/v) sodium citrate. The absorbance of each sample was measured at 412 nm using a blank reagent. A series of GSH solutions in the concentrations range of 10-50 µg were processed simultaneously to generate a standard curve. The amount of GSH in the sample was compared with the standard curve and expressed as µmole/mg protein.

Lipid peroxidation using Thiobarbituric Acid Reactive Substrate (TBARS) assay: Lipid peroxidation in the liver tissue was estimated following the method (TBARS assay) described by Ohkawa et al [26]. The assay is based on the reaction between thiobarbituric acid and Malondialdehyde (MDA), a secondary product of lipid peroxidation at pH 4. The reddish-pink color produced is measured at 532 nm (indicative of the extent of peroxidation). Briefly, 1.5 mL of 20% acetic acid, 0.2 mL of 8.1% Sodium Dodecyl Sulphate (SDS) and 1.5 mL of 8% thiobarbituric acid were added to 0.2 mL of tissue homogenate. The volume of the mixture was adjusted to 4 mL with distilled water and heated at 95°C in a water bath for 60 min. The tubes were cooled to room temperature (25°C) under running water and the final volume was 5 ml in each tube. Five milliliters of a butanol: pyridine (15:1 ratio) mixture

was added and the contents were vortexed thoroughly for 2 min. After centrifugation at 3000 RPM for 10 min (Beckman XL-100 K, USA), the upper organic layer was collected and its absorbance was measured at 532 nm wavelength using spectrophotometer (2800 Unico spectrophotometer USA) against an appropriate reagent blank using a molar extinction coefficient of 1.56 × 105 $M^{-1}cm^{-1}$. The extent of lipid peroxidation is expressed as nmol/g protein.

Histopathological analysis

Fresh portions of the liver were rapidly excised from each rat, washed in 1% ice-cold saline solution and fixed in 10% neutral buffered formalin. Fixed tissues were dehydrated using different grades of ethanol (70%, 80%, 90%, 95% and 100%). Dehydration was performed by clearing the samples with two changes of xylene. The tissue samples were then impregnated with three changes of molten paraffin wax, embedded and blocked. The paraffin blocks were sliced into ribbons of 4 µm thick sections using a Microm HM 360 microtome and mounted on a glass microscope slide. Slides were stained with Hematoxylin and Eosin (H&E) using a Microm HMS-70 Stainer and examined under Nikon eclipse E 800 microscope at x400 magnification. The extent of tissue injury was estimated semi-quantitatively and lesions scored as multi-focal fibrosis/necrosis. At least 5 slides of each sample were scored for liver histology. The liver morphology scored as follows: 0=normal, 1=mild cellular disruption in less than 25% of field area, 2=moderate cellular disruption and hepato cellular vacuolation greater than 50% of field area, 3=extensive cell disruption, hepato cellular vacuolation and condensed nuclei (pycknotic) of hepatocytes in greater than 50% of field area, 4=extensive cell disruption, hepato cellular vacuolation, pycknotic and occasional central vein injury and 5=extensive cell disruption, multi central vein necrosis and degenerating of liver in more than 50% of field area.

Statistical analysis

Statistical analysis was performed with SAS 9.1 software for Windows XP. Data was presented as Means ± SDs. One-way analysis of variance (ANOVA) with p-values less than 0.05 were considered as statistically significant. Dunnett T-Test was used for post hoc evaluation of the data.

Results

Nanomaterial characterization

Nanoparticles were characterized by TEM with respect to morphology, diameter, tendency of aggregation and cellular distribution. Ag-NPs were mainly spherical shaped (Figure 1). To understand the state of dispersion of the particles when placed into deionized water (DI-water), the Ag-NPs sample was analyzed by Dynamic Light Scattering (DLS). The results from DLS showed agglomeration of Ag-NPs more than its primary size (Figure 2A) and the zeta potential value of Ag NPs was shown to be -33.2 mV Figure 2B. A solution is considered stable if the zeta potential value is more negative than -30 mV or more positive than +30 mV.

Effects of Ag-NPs and or Qur on liver enzyme function

Rats treated with 100 mg/kg Ag-NPs for five days exhibited a significant increase in the activities of serum ALT (Figure 3), GGT (Figure 4) and ALP (Figure 5) compared with those in the control group. However, treatment of Ag-NPs treated rats with Qur (Ag-NP+Qur) resulted in a considerable decrease in the activities of serum ALT, GGT and ALP relative to that in the Ag-NPs group. The optical density readings that were obtained for

ALT is as follows 0.277+0.02, 0.632+0.05, 0.311+0.011 for control, 100 mg/kg Ag-NP and 100 mg/kg Ag-NPs+100 µl Qur. For GGT, the optical density reading was 0.277+0.02, 0. 727+0.016, 0.311+0.011 and for ALP optical density readings was 0.277+0.02, 0.447+0.035, 0.311+0.011 respectively. The results obtained from the analysis of liver enzymes have shown that both ALT and GGT had a two-fold increase in the activities in Ag-NPs treated rats relative to the control rats. Furthermore, ALP activity in Ag-NPs treated rats increased compared to that in control rats, however it was not a two-fold increase. In addition, coadministration of Qur to Ag-NPs treated rats showed decrease in all the three liver enzymes (ALT, GGT and ALP) activities compared to Ag-NPs treated rats (Figures 3-5).

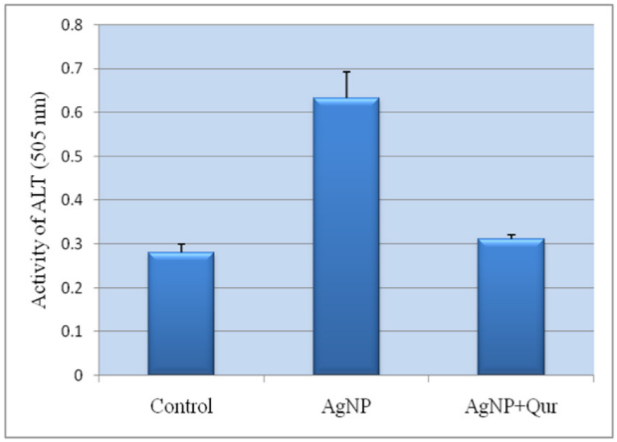

Figure 3) *Effect of silver nanoparticle on the activity of alanine (ALT) aminotransferases in rats.*

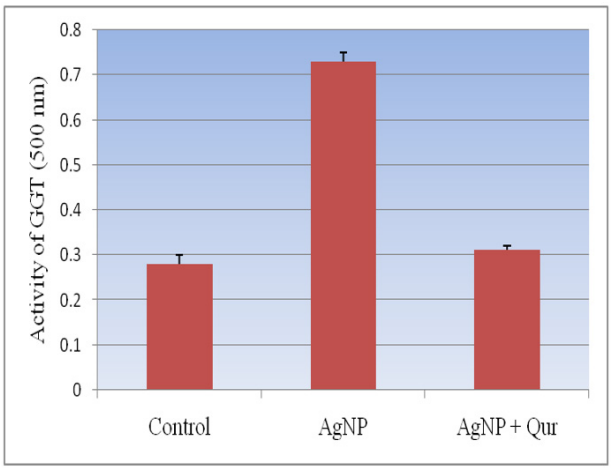

Figure 4) *Effect of silver on the activity of gamma - glutamyl (GGT) aminotransferases in rats.*

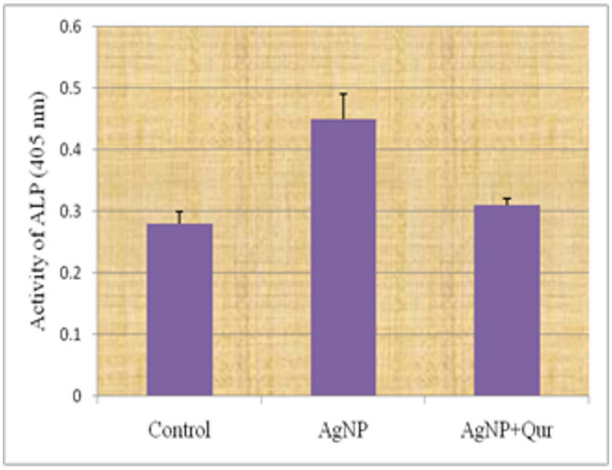

Figure 5) *Effect of silver nanoparticle on the activity of alkaline phosphatases in rats.*

Notes: Figure 3 shows a disturbance in liver ALT and a significant (P<0.05) increase in the Ag-NPs group as compared to control group, while co-administration of Qur along with Ag-NPs significantly decreased the ALT activity respectively.

Notes: Figure 4 shows a disturbance in liver GGT and a significant (P<0.05) increase in the Ag-NPs group as compared to control group, while co-administration of Qur along with Ag-NPs significantly decreased the GGT activity respectively.

Notes: Figure 5 shows a disturbance in liver ALP and an increase in the Ag-NPs group as compared to control group, while co-administration of Qur along with Ag-NPs significantly decreased the ALP activity respectively.

Effect of Ag-NPs and/or Qur on oxidative stress in the liver

Rats exposed to Ag-NPs showed a substantial increase in liver MDA/LPO and a substantial decrease in GSH content compared to those in the control group (Figures 6,7A and 7B). In contrast, the rats treated with Ag-NP along with Qur (Ag-NP+Qur) exhibited a significant decrease in LPO/MDA level and a notable increase in the liver GSH content relative to that in the Ag-NP- exposed group. The MDA

level in the liver homogenate were 18.6+0.57, 42.6+2.00 and 19.4+0.53 for control, Ag-NPs and Ag-NP+Qur respectively. The GSH content were as follows 1.88+0.04, 1.24+0.19, 2. 63+0.02 for control, Ag-NPs and Ag-NP+Qur respectively (Figures 6,7A and 7B).

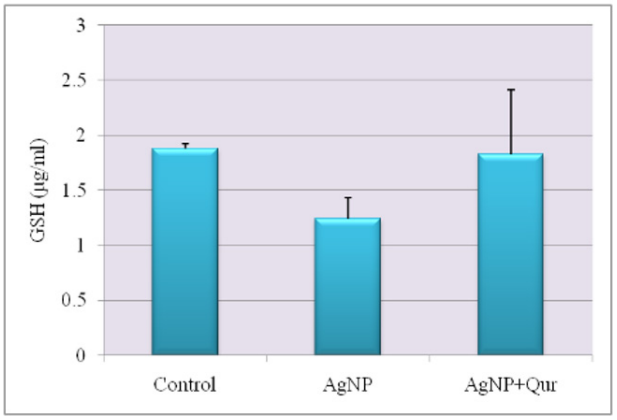

Figure 6) *Effect of silver nanoparticle on the activity of GSH in rats.*

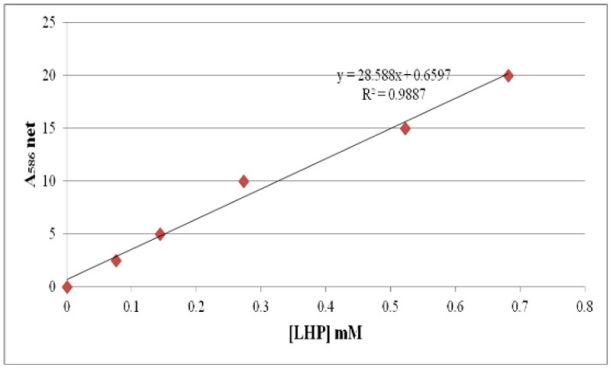

Figure 7A) *Standard curve for LHP/MDA.*

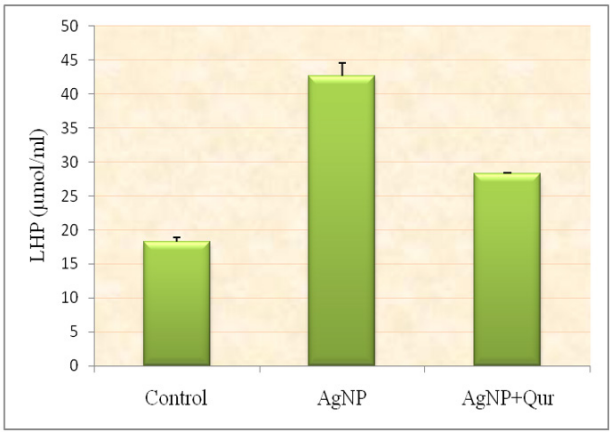

Figure 7B) *Effect of Ag-NPs on the concentration of lipid hydroperoxide (LHP)/MDA in rats.*

Notes: Figure 6 shows oxidative stress alterations in GSH liver homogenate level, where a significant reduction in the Ag-NPs group as compared to control group was observed, while the coadministration of Qur with Ag-NPs significantly increased the GSH respectively.

Notes: Figure 7A shows the level of LHP/MDA in rat liver. MDA level increased significantly in the Ag-NPs group relative to control group, while the coadministration of Qur with Ag-NPs significantly decreased the lipid peroxidation MDA activity respectively.

Effect of Ag-NPs and/or Qur on liver histopathology

Liver section from the control group revealed a normal hepatocyte structure, the hepatocytes were polygonal in shape, with eosinophilic granular cytoplasm and vesicular basophilic nuclei. The liver section of rats exposed to 100 mg/kg Ag-NPs showed diverse histopathological lesions and alteration in the morphology of liver (Figure 8) with diffused infiltration of inflamed cells, such as vacuolated hepatocytes and degeneration with necrosis. The liver sections of rats exposed Ag-NPs+Qur showed an improvement in the hepatocyte's morphology (Figure 8).

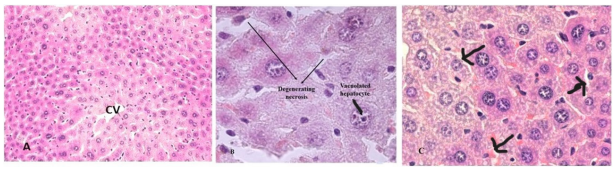

Figure 8) *Rat liver section photos of control and different experimental group stained with hematoxylin & eosin.*

Notes: Figure 8A- Liver section of control group showing normal structure of hepatocytes and central veins (CV), Figure 8B- Liver section of rats treated with 100mg/kg Ag-NPs showing vacuolated hepatocytes and degeneration with focal area, focal necrosis and Figure 8C– Liver sections in Ag-NPs+Qur revealed few atrophied and /or vacuolated hepatocytes and mild infiltration of inflammatory (Black arrows) cells.

Discussion

This study highlights the hepatotoxic effects induced by oral administration of Ag-NPs, as evidenced by the significant increase in the activities of liver enzymes, including ALT, GGT and ALP. Furthermore, Ag-NPs caused a significant increase in lipid peroxidation MDA, alterations in liver morphology and a marked decrease in the oxidative stress biomarker GSH. Treatment with Qur reduced ALT, GGT, ALP and MDA levels. Although GSH increased following Qur treatment, lipid peroxidation and inflammatory liver damage induced by Ag-NPs improved. Despite the increase in biomedical applications of Ag-NPs, their use is limited because of a lack of understanding of the interaction between Ag-NPs and various cellular processes [27]. Oxidative stress due to the excessive production of Reactive Oxygen Species (ROS) and the resulting liver damage have been the subjects of recent studies concerning the cellular targets of Ag-NPs, including induction of the cell death pathway. Following exposure, Ag-NPs are absorbed, enter circulation and are deposited in predominantly in liver.

The by-products of biological aerobic metabolism are known as Reactive Oxygen Species (ROS) including oxygen ions, peroxides and oxygenated free radicals [28]. ROS has been implicated in the toxicity of Ag-NPs by various authors including our previous published study where the highest two doses 50 mg/kg and 100 mg/kg showed statistically significant effect in elevating the induction of ROS relative to the control group [29,30]. However, comparing the two highest doses there was no statistically remarkable outcome in induction of ROS. The results from our previous work demonstrated that an increase in ROS level with an increase in dose of nanoparticles induced oxidative stress [20]. Similar outcome in the toxicity of various nanoparticles have been reported and that non-specific oxidative stress is one of the largest concerns in nanoparticle induced toxicity. ROS are well known to play both a deleterious and beneficial role in biological interactions. In addition, the harmful effects of ROS on the cell include DNA damage, oxidation of lipids, amino acids. Since most chemicals are metabolized in the liver, hepatocytes are targets for ROS. A free radical attack results in lipid peroxidation, which can be linked to the electron transport chain of chemical metabolism and potentially hepatotoxicity. The bioactivity of Qur is related to its high antioxidant and free radical scavenging activities. The antioxidant potential of Qur in the suppression of nanoparticle-induced oxidative stress has been examined using different models. Similar outcomes of Qur have been observed in our present study.

In the present study, administration of 100 mg/kg Ag-NPs caused liver damage, as evidenced by changes in the levels of serum liver enzymes, oxidative stress and histopathology. These findings are in accordance with those reported by us previously [20,31]. The results of our previous study demonstrated that oral administration of Ag-NPs in rats (50 mg/Kg and 100 mg/Kg) significantly enhanced liver enzyme activity and oxidative stress biomarkers relative to that in the control group. These findings indicate that the liver is the target organ for Ag-NPs toxicity, which causes destruction of hepatocyte membranes. Our results are also consistent with the results of other studies that revealed that the over production of metal oxide nanoparticle exposure may cause liver damage [31,32].

Hence, in this study, the potential role of Qur in protecting against Ag-NP-induced cell death pathways and oxidative stress in rats was examined using various assays.

The results revealed that Qur mediated the protective mechanism by reducing the levels of inflammatory mediators and improving liver and organ function. In this study, the simultaneous administration of Qur along with Ag-NPs effectively prevented Ag-NPs-induced inflammatory liver damage. These results are also consistent with previous reports, which demonstrated that Qur decreased inflammation by preventing oxidative stress and production of cytokines [33-35]. These data suggest that Qur has anti-inflammatory effects *in vivo* models.

Size plays a significant role in toxicity of NPs. Gliga et al. found that Ag-NPs measuring 10 nm in diameter were toxic, whereas 40-75 nm Ag-NPs were not toxic [36]. Similar results were reported by Park et al. who demonstrated that Ag-NPs measuring 4 nm caused increased production of Reactive Oxygen Species (ROS) and proinflammatory cytokines in immune cells, unlike Ag-NPs measuring 20-70 nm [37]. Consistent with previous studies, Ag-NPs measuring 10 nm in diameter caused liver damage in this study. Elevated levels of liver enzymes (ALT, GGT, ALP) are key indicators of liver injury. A potential mechanism for liver injury is the aggregation of Ag^{+} in the hepatocytes, which results in generation of excessive amounts of ROS, compromising functional integrity of the hepatocyte membrane. This subsequently contributed to the leakage of enzymes into the blood, thus impairing the liver. However, administration of Qur to Ag-NPs-treated rats decreased the serum levels of ALT, GGT, ALP relative to that in the control rats. The results of this study indicate the ability of Qur to protect against Ag-NPs-induced hepatotoxicity, which is consistent with the results of several previous reports [14,15,18,19,32].

In the current study, after five days of exposure to Ag-NPs, a significant increase in MDA levels and a significant decrease in reduced GSH content were observed in liver tissue in rats. These results demonstrate that Ag-NPs may cause oxidative stress through ROS-mediated process, due to release of silver ions inside the cells, as reported in previous studies [38,39]. The studies found that oxidative stress-related gene expression and biochemical markers in the myelin membranes were altered in Ag-NPs treated rats. Reduction in GSH has a noticeable effect on lipid peroxidation. Primarily, this disruption is improved by Qur treatment. The free radical scavenging activity of Qur has been previously documented. The bioactivity of Qur is associated with high antioxidant activity [12,13].

Conclusion

In summary, short-term and high dose of Ag-NPs in rats induced hepatotoxicity through the mechanism of oxidative stress. An increase in serum liver enzymes activities, increase in level of MDA along with a reduction in GSH content and increase in morphological changes in liver tissue of treated rats was noticed compared to control rats. However, co-administration of 100 µl of Qur to Ag-NPs treated rats ameliorated the Ag-NPs-induced changes, indicating its hepatoprotective activity. The outcome of our present study does not implicate that Ag-NPs should be prohibited for biomedical use, nonetheless, further toxicological studies *in vivo* must be developed to evaluate the toxic effects of nanoparticles.

Acknowledgment

This research was funded by the National Institutes of Health (Grant # U54 MD015929) through the RCMI Center for Environmental Health at Jackson State University, MS, USA.

References

1. Skvortsov AN, Ilyechova EY, Puchkova LV. Chemical background of silver nanoparticles interfering with mammalian copper metabolism. J Hazard Mater. 2023;451:131093.
2. Singh SP, Bhargava CS, Dubey V, et al. Silver nanoparticles: biomedical applications, toxicity, and safety issues. Int J Res Pharm Pharm Sci. 2017;4:1-10.
3. De Souza TA, Souza LR, Franchi LP. Silver nanoparticles: an integrated view of green synthesis methods, transformation in the environment, and toxicity. Ecotoxicol Environ Saf. 2019;171:691-700.
4. Medici S, Peana M, Nurchi VM, et al. Medical uses of silver: history, myths, and scientific evidence. J Med Chem. 2019;62:5923-43.
5. Xu L, Wang YY, Huang J, et al. Silver nanoparticles: synthesis, medical applications and biosafety. Theranostics. 2020;10:8996.
6. Naguib M, Mahmoud UM, Mekkawy IA, et al. Hepatotoxic effects of silver nanoparticles on *Clarias gariepinus*; biochemical, histopathological, and histochemical studies. Toxicol Rep. 2020;7:133-41.
7. Loeb WF, Quimby FW. The clinical chemistry of laboratory animals. Taylor & Francis, Philadelphia, PA. 1999.
8. Zimmerman HJ, Seef LB. Enzymes in hepatic disease. In: Coodley EL, ed. Diagnostic Enzymology. Lea & Febiger, Philadelphia, USA. 1970:1-38.
9. De Maglie M, Cella C, Bianchessi S, et al. Dose and batch-dependent hepatobiliary toxicity of 10 nm silver nanoparticles after single intravenous administration in mice. Int J Health Anim Sci Food Safety. 2015;10:13130.
10. Recordati C, De Maglie M, Bianchessi S, et al. Tissue distribution and acute toxicity of silver after single intravenous administration in mice: nano-specific and size-dependent effects. Part Fibre Toxicol. 2015;13:1-7.
11. Heydarnejad MS, Yarmohammadi-Samani P, Dehkordi MM, et al. Histopathological effects of nanosilver (Ag-NPs) in liver after dermal exposure during wound healing. Nanomed J. 2014;1:191-7.
12. Sadauskas E, Wallin H, Stoltenberg M, et al. Kupffer cells are central in the removal of nanoparticles from the organism. Part Fibre Toxicol. 2007;4:1-7.
13. Mihailovic V, Katanic Stankovic JS, Selakovic D, et al. An overview of the beneficial role of antioxidants in the treatment of nanoparticle-induced toxicities. Oxid Med Cell Longev. 2021:7244677.
14. Fadda LM, Hagar H, Mohamed AM, et al. Quercetin and idebenone ameliorate oxidative stress, inflammation, DNA damage, and apoptosis induced by titanium dioxide nanoparticles in rat liver. Dose Response. 2018;16:1559325818812188.
15. Bhat IU, Bhat R. Quercetin: a bioactive compound imparting cardiovascular and neuroprotective benefits: scope for exploring fresh produce, their wastes, and by-products. Biol. 2021;10:586.
16. Alidadi H, Khorsandi L, Shirani M. Effects of quercetin on tubular cell apoptosis and kidney damage in rats induced by titanium dioxide nanoparticles. Malays J Med Sci. 2018;25:72.
17. Khorsandi L, Orazizadeh M, Moradi-Gharibvand N, et al. Beneficial effects of quercetin on titanium dioxide nanoparticles induced spermatogenesis defects in mice. Environ Sci Pollut Res. 2017;24:5595-606.
18. Arafa AF, Ghanem HZ, Soliman MS, et al. Modulation effects of quercetin against copper oxide nanoparticles-induced liver toxicity in rats. Egypt Pharm J. 2017;16:78-86.
19. Lotfy MM, Ibrahim AI, Saleh YS, et al. Protective role of qurecitin against zinc oxide nanoparticles induced hepatotoxicity. Biochem Lett. 2017;13:30-9.

20. Patlolla AK, Hackett D, Tchounwou PB. Silver nanoparticle-induced oxidative stress-dependent toxicity in Sprague-Dawley rats. Mol Cell Biochem. 2015;399:257-68.

21. Louhimies S. Directive 86/609/EEC on the protection of animals used for experimental and other scientific purposes. Altern Lab Anim. 2002;30:217-9.

22. Giles AR. Guidelines for the use of animals in biomedical research. Thromb Haemost. 1987;58:1078-84.

23. Reitman S, Frankel S. A colorimetric method for the determination of serum glutamic oxalacetic and glutamic pyruvic transaminases. Am J Clin Pathol. 1957;28:56-63.

24. Kay HD. Plasma phosphatase: I. Method of determination. Some properties of the enzyme. J Biol Chem. 1930;89:235-47.

25. Ellman GL. Tissue sulfhydryl groups. Arch Biochem Biophys. 1959;82:70-7.

26. Ohkawa H, Ohishi N, Yagi K. Assay for lipid peroxides in animal tissues by thiobarbituric acid reaction. Anal Biochem. 1979;95:351-8.

27. Rajan R, Huo P, Chandran K, et al. A review on the toxicity of silver nanoparticles against different biosystems. Chemosphere. 2022;292:133397.

28. Prasad S, Gupta SC, Tyagi AK. Reactive Oxygen Species (ROS) and cancer: role of antioxidative nutraceuticals. Cancer Lett. 2017;387:95-105.

29. Mao BH, Chen ZY, Wang YJ, et al. Silver nanoparticles have lethal and sublethal adverse effects on development and longevity by inducing ROS-mediated stress responses. Sci Rep. 2018;8:2445.

30. Nayak D, Kumari M, Rajachandar S, et al. Biofilm impeding AgNPs target skin carcinoma by inducing mitochondrial membrane depolarization mediated through ROS production. ACS Appl Mater Interfaces. 2016;8:28538-53.

31. Heydrnejad MS, Samani RJ, Aghaeivanda S. Toxic effects of silver nanoparticles on liver and some hematological parameters in male and female mice (*Mus musculus*). Biol Trace Elem Res. 2015;165:153-8.

32. Albrahim T, Alonazi MA. Role of beetroot (*Beta vulgaris*) juice on chronic nanotoxicity of silver nanoparticle-induced hepatotoxicity in male rats. Int J Nanomedicine. 2020:3471-82.

33. Abdelhalim MA, Moussa SA, Qaid HA. The protective role of quercetin and arginine on gold nanoparticles induced hepatotoxicity in rats. Int J Nanomedicine. 2018:2821-5.

34. Abdelhalim MA, Moussa SA, Qaid HA, et al. Potential effects of different natural antioxidants on inflammatory damage and oxidative-mediated hepatotoxicity induced by gold nanoparticles. Int J Nanomedicine. 2018:7931-8.

35. Abdelazeim SA, Shehata NI, Aly HF, et al. Amelioration of oxidative stress-mediated apoptosis in copper oxide nanoparticles-induced liver injury in rats by potent antioxidants. Sci Rep. 2020;10:10812.

36. Gliga AR, Skoglund S, Odnevall WI, et al. Size-dependent cytotoxicity of silver nanoparticles in human lung cells: the role of cellular uptake, agglomeration and Ag release. Part Fibre Toxicol. 2014;11:1-7.

37. Park J, Lim DH, Lim HJ, et al. Size dependent macrophage responses and toxicological effects of Ag nanoparticles. Chem Comm. 2011;47:4382-4.

38. Hassanen EI, Khalaf AA, Tohamy AF, et al. Toxicopathological and immunological studies on different concentrations of chitosan-coated silver nanoparticles in rats. Int J Nanomedicine. 2019:4723-39.

39. Dabrowska-Bouta B, Sulkowski G, Struzynski W, et al. Prolonged exposure to silver nanoparticles results in oxidative stress in cerebral myelin. Neurotox Res. 2019;35:495-504.